Electrocatalysis

International Edition: DOI: 10.1002/anie.201511621
German Edition: DOI: 10.1002/ange.201511621

Electrocatalytic Hydrogen Production by a Nickel(II) Complex with a Phosphinopyridyl Ligand

*Ryo Tatematsu, Tomohiko Inomata, Tomohiro Ozawa, and Hideki Masuda**

Abstract: *A novel nickel(II) complex $[Ni(L)_2Cl]Cl$ with a bidentate phosphinopyridyl ligand 6-((diphenylphosphino)-methyl)pyridin-2-amine (L) was synthesized as a metal-complex catalyst for hydrogen production from protons. The ligand can stabilize a low Ni oxidation state and has an amine base as a proton transfer site. The X-ray structure analysis revealed a distorted square-pyramidal Ni^{II} complex with two bidentate L ligands in a trans arrangement in the equatorial plane and a chloride anion at the apex. Electrochemical measurements with the Ni^{II} complex in MeCN indicate a higher rate of hydrogen production under weak acid conditions using acetic acid as the proton source. The catalytic current increases with the stepwise addition of protons, and the turnover frequency is 8400 s^{-1} in 0.1 M $[NBu_4][ClO_4]$/MeCN in the presence of acetic acid (290 equiv) at an overpotential of circa 590 mV.*

Hydrogen produces only water vapor during combustion. It has thus attracted attention as a clean energy and renewable fuel which will provide an important contribution to the resolution of environmental problems.[1,2] Although it is well known that platinum is an excellent catalyst for hydrogen production, it is expensive and has low abundance.[3] In nature, hydrogenase enzymes act as effective catalysts in a reversible two-electron redox reaction of hydrogen at ambient temperature and pressure.[4,5] In particular, [FeFe]-hydrogenase, which includes two iron atoms as the central metals, produces molecular hydrogen with a turnover frequency (TOF) of 6000–9000 s^{-1}.[6] Structural and functional studies of the active sites of [FeFe]hydrogenase have led to the understanding that the highly efficient catalytic activity is provided by proton trapping and the provision of sites near the active center, as well as a hydride-ion interaction site at the iron center.[7] More recently, hydrogen generation by hydrogenase model complexes using inexpensive metals such as iron, cobalt, and nickel have also been investigated.[8,9a,b]

For example, DuBois and co-workers have reported electrochemical hydrogen production using a mononuclear nickel complex bearing a pendant amine as a proton capture site, which has high catalytic activity over TOF = 100 000 s^{-1}.[8a,b] However, this reaction requires strong acid conditions using $[(DMF)H]^+$ ($pK_a = 6.1$ in MeCN) as the proton source and a much higher overpotential of circa 600 mV. Use of a strong acid often induces a decomposition of the molecular catalyst, which is disadvantageous to its durability.

Jones and co-workers have succeeded in developing a nickel complex with an S_2P_2-type ligand bearing a ferrocene substituent and have achieved electrochemical hydrogen production under weak acid conditions with acetic acid ($pK_a = 22.48$ in THF).[9a] Although its overpotential is only 265 mV, its TOF is low (1240 s^{-1}) and thus further improvement of this catalyst is required.

To prepare metal complexes that generate H_2 with a high TOF under weak acid conditions, we designed a new metal complex according to the following design considerations (Scheme 1): 1) a lower valent metal center stabilized using a ligand with π-back-donating character, such as a phosphorus atom, was employed; 2) to stabilize the complex under acidic conditions, we employed a neutral pyridyl nitrogen derivative (which is a borderline base according to the hard and soft acids and bases (HSAB) principle)[17] because it should stabilize the Ni^{II} complex (which is a borderline acid); 3) proton transfer (donor/acceptor) sites, such as an amine, were introduced into the ligand (additionally, it is expected that the hydride complex of the reaction intermediate is stabilized by hydrogen bonding with the amine in the second coordination sphere); and 4) a Ni^{II} ion was selected as the central metal to provide an unsaturated complex with space for the coordination of a hydride.

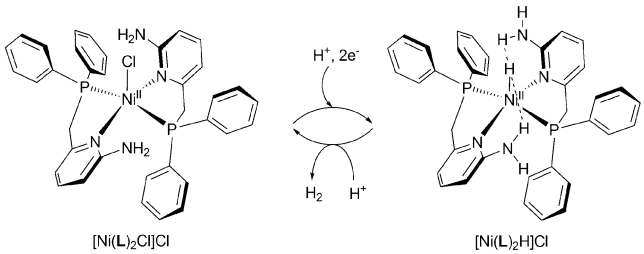

Scheme 1. Proposed mechanism for catalytic H_2 generation in this study.

In this Communication, we report the synthesis and characterization of a novel Ni^{II} complex $[Ni(L)_2Cl]Cl$ containing a bidentate phosphinopyridyl ligand 6-((diphenylphosphino)methyl)pyridin-2-amine (L) and investigate its catalytic properties with respect to electrochemical hydrogen production.

The synthesis of ligand L was performed according to the method shown in Scheme 2. The amine group of 2-amino-6-methylpyridine was protected by reacting with pivaloyl

[*] R. Tatematsu, Prof. T. Inomata, Prof. T. Ozawa, Prof. H. Masuda
Department of Frontier Materials
Graduate School of Engineering, Nagoya Institute of Technology
Gokiso, Showa, Nagoya 466–8555 (Japan)
E-mail: masuda.hideki@nitech.ac.jp

Supporting information for this article can be found under: http://dx.doi.org/10.1002/anie.201511621.

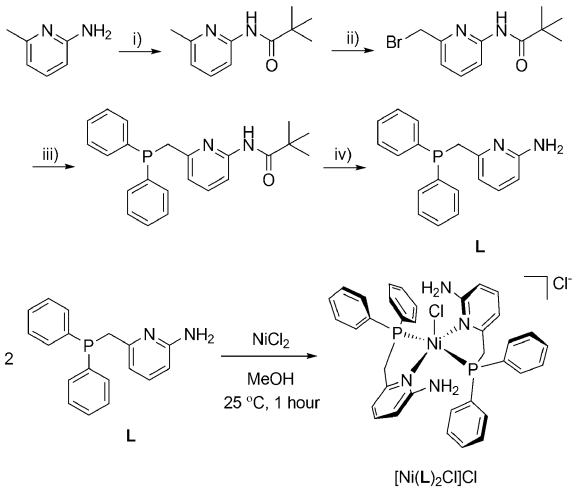

Scheme 2. Preparation of ligand L and Ni^{II} complex $[Ni(L)_2Cl]Cl$. Conditions: i) pivaloyl chloride, Et_3N, CH_2Cl_2, 0 °C, 4 h; ii) NBS, AIBN, CCl_4, 70 °C, 6 h; iii) Ph_2PH, *t*-BuOK, 25 °C, 24 h; iv) KOH, MeOH, 60 °C, 1 week. NBS = *N*-bromosuccinimide; AIBN = azobisisobutyronitrile.

chloride and then the methyl group was brominated. The resulting 2-pivaloylamino-6-bromomethylpyridine was treated with diphenylphosphine under basic conditions to afford an amine-protected precursor. Ligand L was obtained by hydrolyzing the pivalamide group under strongly basic conditions. The details of the synthesis and assignment of its ^1H NMR spectrum are described in the Supporting Information. Addition of 2 equiv of L to a MeOH solution of anhydrous $NiCl_2$ changes the solution color from yellow to purple/red. Fortunately, we obtained a purple/red single crystal suitable for X-ray analysis by recrystallization of the complex upon addition of Et_2O to the MeOH solution. The complex was characterized by elemental analysis, IR spectroscopy, and X-ray crystallography in the solid state and UV/Vis spectroscopy in the solution state.

X-ray structural analysis (Figure 1) revealed that the Ni^{II} complex forms a slightly distorted square-pyramidal geometry with two bidentate phosphinopyridyl ligands L in the equatorial plane and a chloride anion at the axial position. The Ni–P bond lengths are Ni–P1 = 2.2214(4) and Ni–P2 = 2.2146(4) Å, and the Ni–N bond lengths are Ni–N1 = 1.9424(13) and Ni–N2 = 1.9471(14) Å. These values are in good agreement with those of a previously reported nickel(II) complex (iodo-bis-[2-(diphenylphosphinomethyl)pyridine]-nickel(II) iodide) with chelating diphenylphosphine (2.163, 2.169 Å) and pyridine ligands (1.956, 1.970 Å), respectively.[11] However, the Ni–Cl bond length (2.737(6) Å) is significantly longer than the previously reported Ni–Cl bond lengths (2.302–2.314 Å), indicating weak binding of Cl^-.[12] The amines interact with the apical chloride atom at a hydrogen bonding distance of $Cl\cdots N(H_2) \approx 3.1$ Å. The distance between the amine and the nickel atom is about 3.1 Å, indicating that both proton transfer sites are positioned near the active site of the metal center. Additionally, the nickel complex can convert into a flexible structure from the planar structure formed by the coordinating atoms of ligand L (P-Ni-P = 148.38°, N-Ni-N = 163.48°) to form a structurally controlled distorted square pyramidal structure (see Equation (S1) in the Supporting Information; $\tau_5 = 0.25$). Interestingly, one of the phenyl rings of the diphenylphosphine interacts with the coordinated pyridine ring in the π–π stacking mode with a separation of about 3.5 Å. This interaction may contribute to the structural stabilization of $[Ni(L)_2Cl]Cl$.

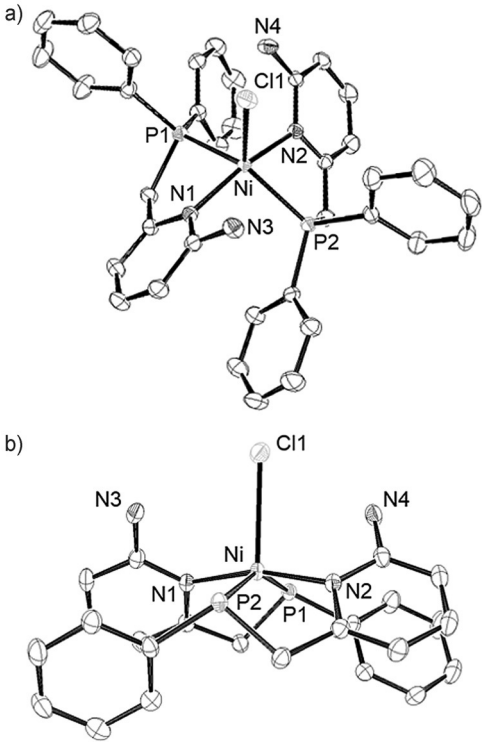

Figure 1. ORTEP view of a) the cation part of $[Ni(L)_2Cl]Cl{\cdot}2\,MeOH$, with thermal ellipsoids set at 50% probability. MeOH solvent molecules, the other chloride ion, and H atoms are omitted for clarity. In side view (b), the other phenyl group is omitted for clarity. Selected distances/bond lengths [Å] and angles [°]: Ni–P1 = 2.2214(4), Ni–P2 = 2.2146(4), Ni–N1 = 1.9424(13), Ni–N2 = 1.9471(14), Ni–Cl1 = 2.737(6), Ni···N3 = 3.1330(14), Ni···N4 = 3.0978(16), N3···Cl1 = 3.1991(16), N4···Cl1 = 3.1079(15); P1-Ni-N1 = 84.18(4), P1-Ni-N2 = 91.81(4), P2-Ni-N1 = 92.63(4), P2-Ni-N2 = 82.39(4), P1-Ni-P2 = 148.38(2), N1-Ni-N2 = 163.48(7).

Electronic absorption spectra (see Figure S1 in the Supporting Information) of the Ni^{II} complex in a range of different solvents show an intense absorption band in the range $\lambda = 488$–508 nm (EtOH: $\lambda = 497$ nm, molar extinction coefficient (ε) = 1917 $M^{-1}cm^{-1}$; MeOH: $\lambda = 488$ nm, ε = 1643 $M^{-1}cm^{-1}$; MeCN: $\lambda = 508$ nm, $\varepsilon = 1700\ M^{-1}cm^{-1}$; and CH_2Cl_2: $\lambda = 501$ nm; $\varepsilon = 1115\ M^{-1}cm^{-1}$). These absorption bands are assigned to d–d transitions ($^1A_1 \rightarrow {}^1E$) originating from a low-spin square-pyramidal Ni^{II} complex.[13] In an aprotic solvent, two additional weak absorption bands were detected in the longer wavelength region, that is, at $\lambda = 903$–905 nm and 1025–1030 nm in MeCN and CH_2Cl_2, respectively. These bands are assigned to d–d transitions ($^3A_{2g} \rightarrow {}^3T_{1g}$ and $^3A_{2g} \rightarrow {}^3T_{2g}$) originating from a six-coordinate octahedral Ni^{II} complex.[14] These findings suggest that the complex is in equilibrium between a pyramidal structure and an octahedral structure with chloride ions weakly bound to the metal center.

In a protic solvent, these absorption bands are not detected, showing that an uncoordinated chloride ion has been stabilized by solvation. The equilibrium behavior was also evident in the ^{1}H NMR spectra (Figures S11 and S12).

Electrochemical measurements (specifically cyclic voltammetry (CV)) of $[Ni(L)_2Cl]Cl$ were carried out in 0.1 M $[NBu_4][ClO_4]$ in MeCN as the supporting electrolyte at a scan rate of 100 mV s^{-1} under an Ar atmosphere. The redox waves attributed to nickel(II/I) and nickel(I/0) redox couples were detected at $E_{1/2} = -0.96$ V ($\Delta E_p = 70$ mV) and $E_{1/2} = -1.48$ V ($\Delta E_p = 170$ mV) versus Fc/Fc$^+$, respectively, in which the former and the latter waves are reversible and irreversible, respectively. A new oxidation wave was generated at the potential of −1.19 V when the sweep rate was increased from 100 to 500 mV s^{-1} (Figure S2). Plots of the reduction current (i_p) versus the square root of the scan rate are linearly correlated (Figure S3), implying that the electrochemical event is diffusion controlled.

The electrocatalytic reduction of protons in the presence of $[Ni(L)_2Cl]Cl$ (1 mM) was evaluated in 0.1 M $[NBu_4][ClO_4]$ in MeCN as the supporting electrolyte under weak acid conditions (Figure 2). The profile of the CV changes significantly when acetic acid is sequentially added as the proton

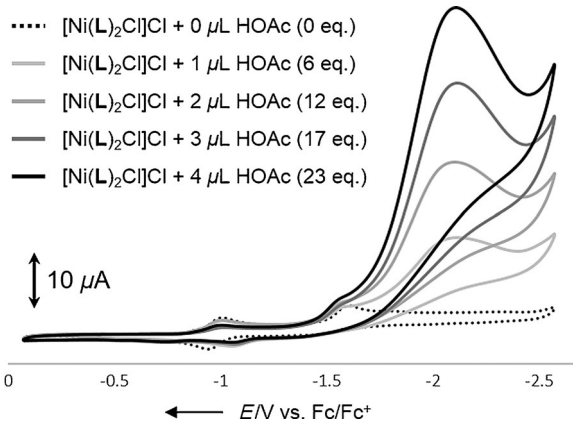

Figure 2. Cyclic voltammograms of $[Ni(L)_2Cl]Cl$ (1 mM) with various amounts of acetic acid added. 0.1 M $[NBu_4][ClO_4]$ in MeCN was employed as the supporting electrolyte; scan rate = 0.3 V s^{-1}.

source to the MeCN solution ($pK_a = 22.3$ in MeCN).[10] The catalytic current (i_{cat}) increases with an increase in the amount of acetic acid added (where the i_{cat} is derived from two-electron reduction of protons, as described below). Additionally, the potentials corresponding to the wave maximum value shift to a more positive region in the presence of the acid, as compared to in the absence of complex.[10] The $Ni^{II/I}$ and $Ni^{I/0}$ reduction potentials do not change under the acidic conditions, showing that catalysis proceeds through an EECC mechanism (two electrons and two chemical steps).[15] These findings suggest that $[Ni(L)_2Cl]Cl$ has reactivity as a catalyst for hydrogen generation.

Next, the changes in the cyclic voltammogram of complex $[Ni(L)_2Cl]Cl$ with larger increases in the acid concentration added were studied by addition of 5 μL (29 equiv) aliquots of acetic acid into the solution (Figure S4). The plots of i_{cat}/i_p versus the square root of the amounts of added acetic acid indicate a linear correlation until approximately 290 equiv (circa 50 μL) of acid have been added (Figure S5). This indicates that the reaction is first order for the acid concentration [Eq. (S4)]. The i_{cat}/i_p value for each aliquot of acid added was measured at the potential where the current has its maximum value. At high acid concentrations (that is, more than 50 μL of acid added), the plots of the i_{cat}/i_p value versus the square root of the amounts of acetic acid added becomes nonlinear (Figure S5), suggesting that the catalyst decomposes in this range.

Figure 3 shows a plot of the amount of added acetic acid versus the k_{obs} values (TOF), calculated from the i_{cat}/i_p ratio using Equation (S6), which reaches a plateau around $k_{obs} = 11\,000$ s^{-1}. In the range where the complex does not decompose, the i_{cat}/i_p value is estimated to be 120.2 when 50 μL

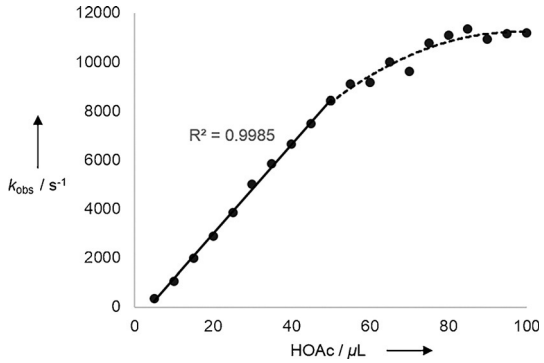

Figure 3. Plots of the calculated k_{obs} value versus the volume of added HOAc for a solution of $[Ni(L)_2Cl]Cl$ (1 mM) in 0.1 M $[NBu_4][ClO_4]$ in MeCN as the supporting electrolyte. Scan rate = 0.3 V s^{-1}.

(290 equiv) of acetic acid is added, corresponding to TOF = 8400 s^{-1}. Under acidic conditions, no increase in the i_{cat} value was detected at scan rates faster than 300 mV s^{-1} (Figures S6 and S7). This suggests that in the range of the scan rates applied, the catalytic process is not a diffusion-controlled reaction. The overpotential value estimated using Equations (S7, S8) is circa 590 mV in the presence of 50 μL (290 equiv) of acetic acid. Hydrogen production was confirmed by gas chromatography (GC) following the controlled potential electrolysis, and its Faradaic efficiency was determined to be 89.8%. Furthermore, controlled potential electrolysis of $[Ni(L)_2Cl]Cl$ (0.5 mM) at −2.5 V versus Ag/Ag$^+$ in the absence of acetic acid indicates a small amount of hydrogen production (detected by GC), suggesting that catalytic hydrogen production might proceed through the basic sites of the amine acting as proton transfer sites.

Electrochemical hydrogen production under weak acid conditions using acetic acid as the proton source has been previously investigated,[9] but an abundant metal catalyst which provides a TOF greater than 8000 s^{-1} is rare.[9a,b] We believe that the electrocatalysis results obtained in this study can be attributed to the effect of the basic sites of the amine based on two key observations: 1) from X-ray structural analysis, the hydride complex of the reaction intermediate is stabilized by hydrogen bonding with the amine (NiH···HN) as

well as between the apical chloride ion and the amine (NiCl···HN); and 2) from the results of controlled potential electrolysis experiments in the absence of acid, catalytic hydrogen production was found to be promoted by proton transfer via the basic sites of the amine. Hydrogen bonding and proton transfer between substrates and ligands in the second coordination sphere have been reported by a number of different research groups and it is clear that these interactions are very important factors in the catalytic reaction.[16] We have succeeded in developing a potent hydrogen-generating metal complex catalyst. However, from the viewpoint of proton reduction, the overpotential is also a very important factor. In the future, further improvement of our catalyst will be necessary to generate hydrogen at a lower overpotential. Additionally, as the contribution of the amine as a proton donor/acceptor site to the catalytic reaction is not fully clear, understanding the function of the amine is currently under consideration.

In summary, a new slightly distorted square-planar Ni^{II} complex $[Ni(L)_2Cl]Cl$ with two bidentate phosphinopyridyl ligands was synthesized and characterized by means of UV/Vis absorption spectroscopy, X-ray structural analysis, and electrochemistry. In the electrochemical reduction of protons, the electrocatalytic currents indicating hydrogen generation were found to increase with an increase in the amounts of acetic acid added. The TOF value evaluated on the basis of the electrochemical reduction is 8400 s^{-1} at an overpotential of circa 590 mV, indicating that the Ni^{II} complex has a high proton-reduction ability even under weak acid conditions. These results will provide the foundation for the development of similar complexes as future hydrogen-generation catalysts.

Acknowledgements

This research was supported by a Grant-in-Aid for Scientific Research from the Ministry of Education, Science, Sports and Culture and from the Program for Advancing Strategic International Network to Accelerate the Circulation of Talented Researchers (JSPS).

Keywords: electrocatalysis · electrochemistry · hydrogen · hydrogenases · nickel

How to cite: *Angew. Chem. Int. Ed.* **2016**, *55*, 5247–5250
Angew. Chem. **2016**, *128*, 5333–5336

[1] J. A. Turner, *Science* **2004**, *305*, 972–974.
[2] R. Eisenberg, D. G. Nocera, *Inorg. Chem.* **2005**, *44*, 6799–6801.
[3] R. M. Bullock, *Catalysis without Precious Metals*, 1st ed., Wiley-VCH, New York, **2010**.
[4] J. C. Fontecilla-Camps, A. Volbeda, C. Cavazza, Y. Nicolet, *Chem. Rev.* **2007**, *107*, 4273–4303.
[5] K. A. Vincent, A. Parkin, F. A. Armstrong, *Chem. Rev.* **2007**, *107*, 4366–4413.
[6] M. Frey, *ChemBioChem* **2002**, *3*, 153–160.
[7] Y. Nicolet, A. L. de Lacey, X. Vernéde, V. M. Fernandez, E. C. Hatchikian, J. C. Fontecilla-Camps, *J. Am. Chem. Soc.* **2001**, *123*, 1596–1601.
[8] a) M. L. Helm, M. P. Stewart, R. M. Bullock, M. Rakowski DuBois, D. L. DuBois, *Science* **2011**, *333*, 863–866; b) D. L. DuBois, *Inorg. Chem.* **2014**, *53*, 3935–3960; c) A. Kochem, F. Thomas, O. Jarjayes, G. Gellon, C. Philouze, T. Weyhermüller, F. Neese, M. van Gastel, *Inorg. Chem.* **2013**, *52*, 14428–14438; d) M. E. Carroll, B. E. Barton, T. B. Rauchfuss, P. J. Carroll, *J. Am. Chem. Soc.* **2012**, *134*, 18843–18852; e) G. P. Connor, K. J. Tribble, W. R. McNamara, *Inorg. Chem.* **2013**, *52*, 14428–14438.
[9] a) L. Gan, T. L. Groy, P. Tarakeshwar, S. K. S. Mazinani, J. Shearer, V. Mujica, A. K. Jones, *J. Am. Chem. Soc.* **2015**, *137*, 1109–1115; b) S. Roy, S. K. S. Mazinani, T. L. Groy, L. Gan, P. Tarakeshwar, V. Mujica, A. K. Jones, *Inorg. Chem.* **2014**, *53*, 8919–8929; c) A. Z. Haddad, D. Kumar, K. O. Sampson, A. M. Matzner, M. S. Mashuta, C. A. Grapperhaus, *J. Am. Chem. Soc.* **2015**, *137*, 9238–9241; d) T. A. White, S. E. Witt, Z. Li, K. R. Dunbar, C. Turro, *Inorg. Chem.* **2015**, *54*, 10042–10048.
[10] G. A. N. Felton, R. S. Glass, D. L. Lichtenberger, D. H. Evans, *Inorg. Chem.* **2006**, *45*, 9181–9184.
[11] V. W. Haase, *Z. Anorg. Allg. Chem.* **1974**, *404*, 273–283.
[12] H.-B. Burgi, J. D. Dunitz, *Structure Correlation*, *Vol. 2*, Wiley-VCH, Weinheim, **1994**.
[13] J. R. Preer, H. B. Gray, *J. Am. Chem. Soc.* **1970**, *92*, 7306–7312.
[14] C. W. Reimann, *J. Phys. Chem.* **1970**, *74*, 561–568.
[15] C. Costentin, J.-M. Savéant, *ChemElectroChem* **2014**, *1*, 1226–1236.
[16] a) A. Wada, M. Harata, K. Hasegawa, K. Jitsukawa, H. Masuda, M. Mukai, T. Kitagawa, H. Einaga, *Angew. Chem. Int. Ed.* **1998**, *37*, 798–799; *Angew. Chem.* **1998**, *110*, 874–875; b) C. M. Moore, D. A. Quist, J. W. Kampf, N. K. Szymczak, *Inorg. Chem.* **2014**, *53*, 3278–3280; c) M. J. Goldcamp, S. E. Robison, J. A. Krause Bauer, M. J. Baldwin, *Inorg. Chem.* **2002**, *41*, 2307–2309; d) C. M. Moore, N. K. Szymczak, *Chem. Commun.* **2013**, *49*, 400–402.
[17] R. G. Pearson, *Coord. Chem. Rev.* **1990**, *100*, 403–425.

Received: December 14, 2015
Revised: February 18, 2016
Published online: March 16, 2016

